East European Journal of Physics. 2. 372-379 (2024)
DOI:10.26565/2312-4334-2024-2-46 ISSN 2312-4334

COMPARISON OF 2D AND 3D P-N JUNCTION DIFFERENTIAL CONDUCTANCE AND DIFFUSION CAPACITANCE

Muhammadjon G. Dadamirzaev, Mamura O. Kosimova*, S.R. Boydedayev, Azamat S. Makhmudov
Namangan Engineering-Construction Institute, Namangan 160103, Uzbekistan
**Corresponding Author e-mail: omamuraqosimova@gmail.com*
Received April 9, 2024; revised April 27, 2024; accepted May 15, 2024

In the fabrication of 3D p-n junctions, doping or surface modification caused by ion injection changes the electrical properties and crystal structure of the semiconductor. In addition, as the size of the semiconductor device decreases, various quantum effects are gradually appearing in them. This shows that the scope of application of classical device theory is now limited. In recent years, two-dimensional (2D) materials with amazing atomically fine properties have attracted great interest. The electrostatic field properties of some 2D p-n junctions, such as WS2, MoS_2, $MoSe_2$, WSe_2, and black phosphorus (BP), open the door to new possibilities for semiconductors. Changes in the diffusion capacitances and differential conductance's of 2D p-n junctions under the influence of an microwave field, and the diffusion capacitances and differential conductance's of 2D and 3D p-n junctions the change of conductivities under the influence of microwave field is compared.
Keywords: *p-n-junction; Diffusion capacitance; Differential conductance; Microwave field; 2D dimensional materials*
PACS: 85.30. Kk

INTRODUCTION

p-n-junction rectifiers consisting of two types of semiconductors [1], photodetectors [1-5], photovoltaics [6-10], and light-emitting diodes [11-12] are the basis of electronic and optoelectronic devices. In the fabrication of 3D p-n junctions, doping or surface modification caused by ion injection changes the electrical properties and crystal structure of the semiconductor. In addition, as the size of the semiconductor device decreases, various quantum effects are gradually appearing in them. This shows that the scope of application of classical device theory is now limited.

In recent years, two-dimensional (2D) materials with amazing atomically fine properties have attracted great interest. The electrostatic field properties of some 2D p-n junctions, such as WS2, MoS_2, $MoSe_2$, WSe_2, and black phosphorus (BP), open the door to new possibilities for semiconductors [9,13-18]. Using light as an external field to diodes provides many additional advantages. For example, light can be sent from a distance. This is of great importance for modern integrated optoelectronic connection circuits that are precisely controlled, fast switching and consume very little energy [19-25].

In [26], the Poisson equation for a 2D p-n junction is combined with the drift-diffusion and continuity equations and the Shockley equation for an ideal current-voltage characteristics is proposed. Fig. 1 shows the geometric scheme of a 2D p-n junction. This structure is formed by the combination of p and n types at x=0 and lies in z=0 plane, the structure along the y axis is large enough, so the effect of this direction on the properties is considered.

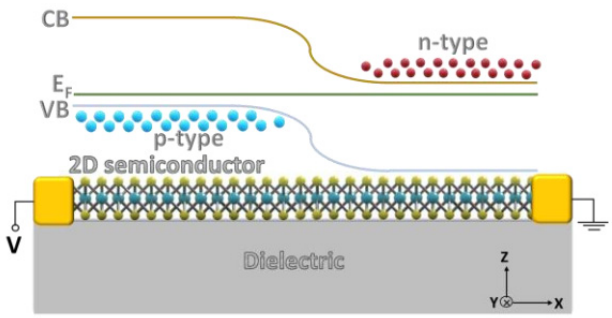

Figure 1. Geometric scheme of 2D p-n junction [26]

Fig. 2 shows the quasi-Fermi levels and energy states obtained in the authors' numerical model for the physical structure of a 2D p-n junction in thermodynamic equilibrium. At equilibrium, φ increases through the filling layer, while at nonequilibrium, φ decreases or increases depending on the direction of the voltage.

In addition, in this work, the recombination and generation processes in the effective depletion layer (EDL) are significantly deviated from the ideal, and the capacitances and conductance of the 2D p-n junction are considered. The

Cite as: M.G. Dadamirzaev, M.O. Kosimova, S.R. Boydedayev, A.S. Makhmudov, 2024; East Eur. J. Phys. 2, 372 (2024), https://doi.org/10.26565/2312-4334-2024-2-46

barrier and diffusion capacities for the structure in the non-equilibrium state were analyzed. The barrier capacity was calculated by the following expression:

$$C_б = \frac{2\pi\varepsilon_{эфф}}{8G}. \quad (1)$$

Diffusion capacity calculated by this expression:

$$C_{df} = \frac{2qn_i(L_p + L_n)\exp\left(\frac{qU}{kT}\right)}{2kT}. \quad (2)$$

Using these expressions, capacitance plots are presented based on the authors' numerical model for a silicon-based 3D p-n junction and a 2D monolayer MoS_2.

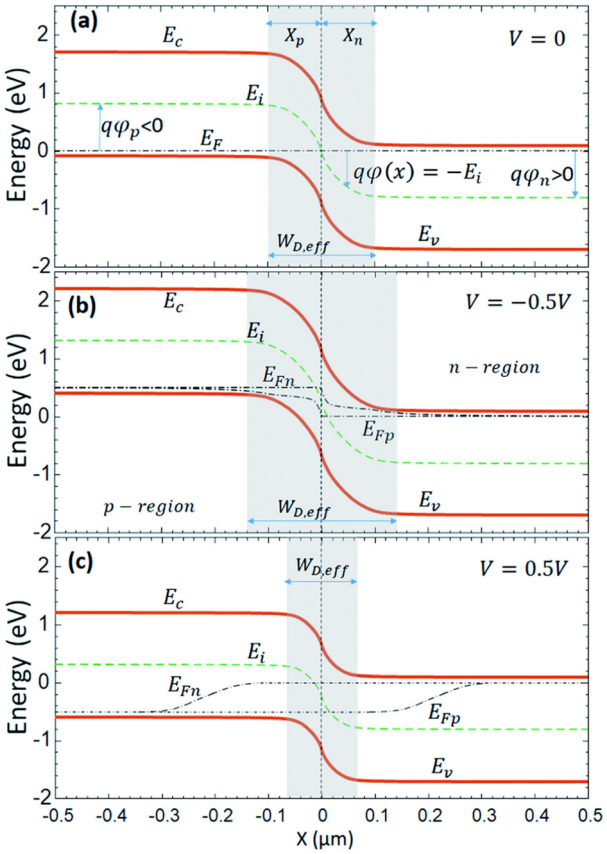

Figure 2. Zone diagram of 2D p-n junction in thermodynamic equilibrium state (a); in the reverse direction (b) and in the forward direction (c) [26]

However, in the above-mentioned studies, the changes of diffusion capacities and differential conductivities of 2D p-n junctions due to external influences have not been sufficiently studied, and the differences between 3D and 2D p-n junctions' graphs of changes of diffusion capacities and differential conductivities as a result of external influences are not compared.

The purpose of the work is to analyze the change of diffusion capacities and differential conductivities of 2D and 3D p-n junctions as a result of external influences.

COMPARISON OF 2D AND 3D p-n JUNCTION DIFFERENTIAL CONDUCTANCE

The differential conductivity of a p-n junction in 3D size is determined by the following relation [27]:

$$G = \frac{eI_s}{kT}\exp\left(\frac{eU}{kT}\right) \quad (3)$$

Differential conductance of p-n junction in 2D size using the expressions presented in the work [27], we get the following formula:

$$G = \frac{q^2 n_i^2}{kTN_d}\left(\frac{D_p}{L_p} + \frac{D_n}{L_n}\right)\exp\left(\frac{qU}{kT}\right), \quad (4)$$

here, $n_i = g_{2D} kT \exp\left(-\frac{E_g}{2kT}\right)$, $L_n = L_p = \sqrt{D_{n(p)}\tau_{n(p)}}$, $D_{n(p)} = \frac{kT\mu_{n(p)}}{q}$, $E_g = 1.8eV$, $\mu_n = \mu_p = 50\frac{sm^2}{Vs}$, $\tau_n = \tau_p = 3\cdot 10^{-10} s$, $n_i = 9.9\cdot 10^{-3} sm^{-2}$.

From the expressions (3) and (4), 2D and 3D p-n junction differential conductivities were compared (Fig. 3).

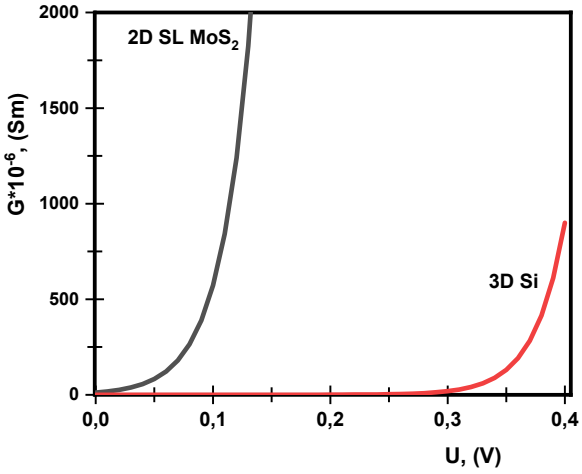

Figure 3. Rate dependence of p-n junction differential conductance in 2D and 3D dimensions

Fig. 3 shows the voltage dependence of the differential conductance of a 2D and 3D p-n junction. The obtained results show that the differential conductance of the 3D p-n junction is smaller than the differential conductance of the 2D p-n junction. This shows that the 2D p-n junction is more efficient than the 3D p-n junction.

Electrons and holes in a 3D p-n junction are not heated under the influence of a weak microwave field, and if only the perturbation of the potential barrier height is taken into account, we have the following expression for the differential conductance of the p-n junction [28]:

$$G = \frac{eI_s}{kT} e^{-\frac{e(U+U_1-\phi_0)}{kT}}. \tag{5}$$

We have the following expression for the differential conductance of a 2D-sized p-n junction under the influence of a weak microwave field:

$$G = \frac{q^2 n_i^2}{kTN_d}\left(\frac{D_p}{L_p} + \frac{D_n}{L_n}\right)\exp\left(\frac{q(U+U_1-\phi)}{kT}\right). \tag{6}$$

Using expressions (5) and (6), it is possible to compare the differential conductivities of 2D and 3D p-n junctions located in a weak microwave field (Fig. 4).

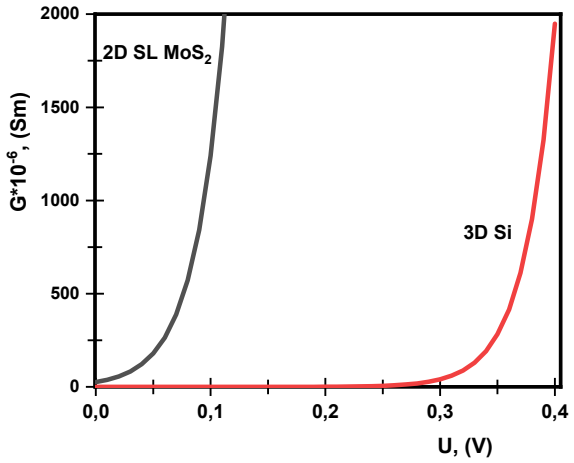

Figure 4. Dependence of applied voltage of the differential conductance of 2D and 3D p-n junctions located in a weak microwave field

Fig. 4 shows the voltage dependence of the differential conductance of a 2D and 3D p-n junction located in a weak microwave field. The obtained results show that the 3D p-n junction differential conductance located in the microwave is smaller than the 2D p-n junction differential conductance. This shows that a 2D p-n-junction located in a weak microwave field is more efficient than a 3D p-n-junction.

We have the following expression for the differential conductance of a 3D-dimensional p-n junction under the influence of a strong microwave field:

$$G = \left(\frac{kT}{eI_e} \sqrt{\frac{T}{T_e}} e^{\left(\frac{e(\phi_0 - U - U_1)}{kT_e} - \frac{e\phi_0}{kT} \right)} + \frac{kT}{eI_h} \sqrt{\frac{T}{T_h}} e^{\left(\frac{e(\phi_0 - U - U_2)}{kT_h} - \frac{e\phi_0}{kT} \right)} \right)^{-1}. \quad (7)$$

We have a differential expression for the differential conductance of a 2D-sized p-n junction under the influence of a strong microwave field:

$$G = \frac{q^2 n_i^2}{kTN_d} \left(\frac{D_p}{L_p} + \frac{D_n}{L_n} \right) \left(\sqrt{\frac{T}{T_e}} \exp\left(\frac{q(\phi - U - U_1)}{kT_e} - \frac{q\phi}{kT} \right) + \sqrt{\frac{T}{T_h}} \exp\left(\frac{q(\phi - U - U_2)}{kT_h} - \frac{q\phi}{kT} \right) \right)^{-1}. \quad (8)$$

Using expressions (7) and (8), it is possible to compare the differential conductivities of 2D and 3D p-n junctions located in a strong UHF field (Fig. 5).

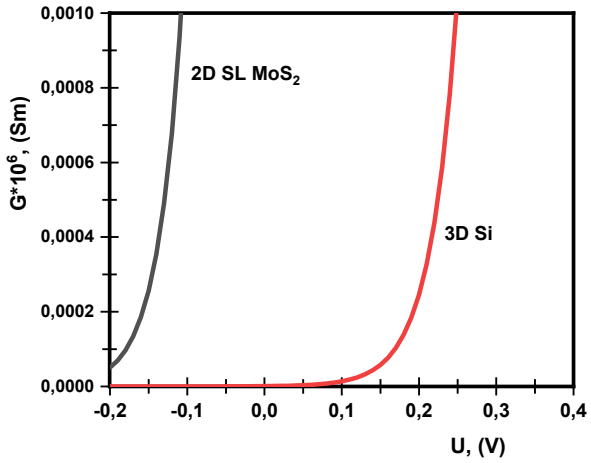

Figure 5. Dependence of differential conductance of 2D and 3D p-n junctions located in a strong microwave field on applied voltage

Figure 5 shows Dependence of differential conductance of 2D and 3D p-n junctions located in a strong microwave field on applied voltage. The obtained results show that the differential conductance of a 3D-sized p-n junction located in a strong microwave field is small compared to the differential conductance of a 2D-sized p-n junction. This shows that the 2D p-n junction located in a strong microwave field is more efficient than the 3D p-n junction.

Using the expressions (4), (6) and (8), the variation of the 2D p-n junction differential conductance without the influence of the microwave field, under the influence of the weak and strong UHF field is shown in Fig. 6.

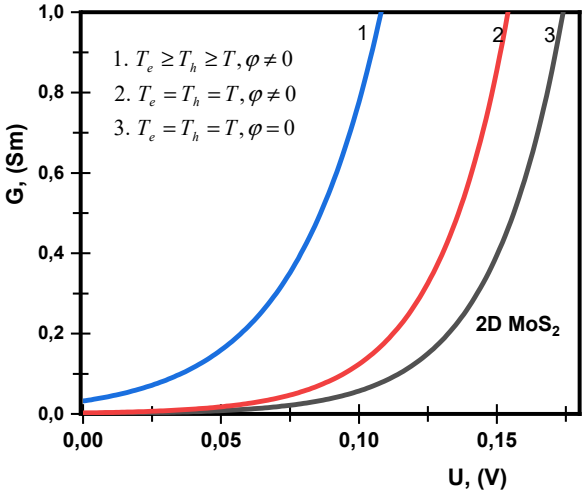

Figure 6. Variation of the differential conductance of a 2D p-n junction under the influence of a strong microwave field

From the obtained results, it can be seen that the differential conductance of the 2D-sized p-n junction increases under the influence of a strong microwave field.

COMPARISON OF DIFFUSION CAPACITIES OF 2D AND 3D p-n JUNCTIONS

For 3D-dimensional p-n junction diffusion capacitance [28]

$$C = \frac{\tau e I_s}{2kT} e^{\frac{eU}{kT}}, \tag{9}$$

using the expression, its graph on a logarithmic scale can be obtained (Fig. 7).

The diffusion capacity of a 2D p-n junction is determined by the following relation [27]:

$$C = \frac{q^2 n_i^2 \left(L_n + L_p\right)}{2kTN_d} \exp\left(\frac{qU}{kT}\right). \tag{10}$$

The graph of expressions (10) and (11) on a logarithmic scale is shown in Figure 8.

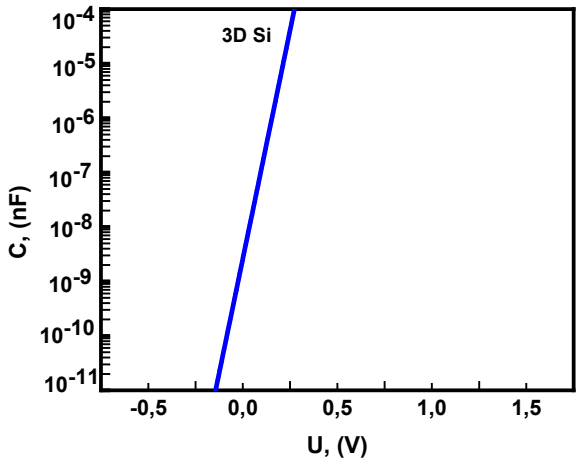

Figure 7. Voltage dependence of the diffusion capacitance for a 3D p-n junction

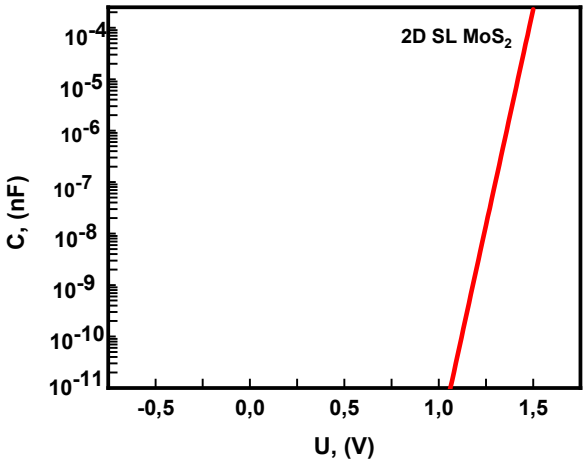

Figure 8. Voltage dependence of diffusion capacity for 2D monolayer SL MoS_2

We compare the diffusion capacities of p-n junctions in 3D and 2D sizes from a theoretical point of view (Fig. 10).

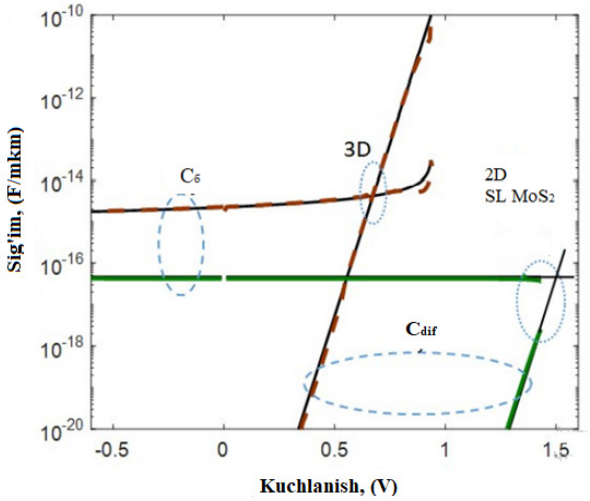

Figure 9. Comparison of barrier and diffusion capacities for silicon-based 3D p-n junction and 2D monolayer MoS_2 [26]

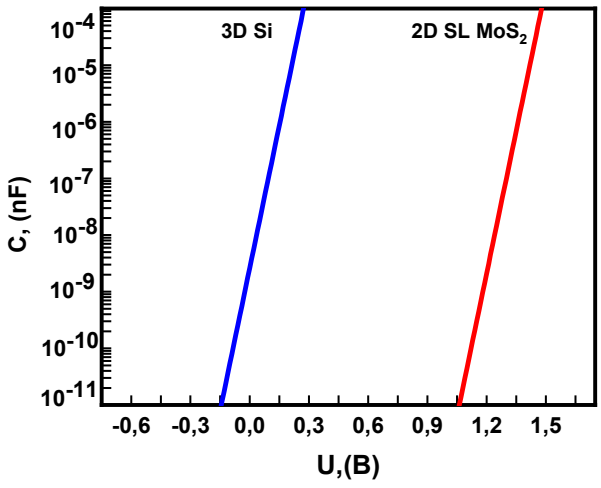

Figure 10. Voltage dependence of p-n junction diffusion capacitance in 3D and 2D dimensions

As can be seen from Figures 9 and 10, the theoretical calculations and experimental results show that the diffusion capacity for 2D monolayer SL MoS_2 is larger than the 3D Si diffusion capacity.

Electrons and holes in a 3D p-n junction are not heated under the influence of a weak microwave field, and we have an expression for the diffusion capacity of a p-n junction when only the perturbation of the potential barrier is obtained [29]:

$$C = \frac{eI_s\tau}{2kT} e^{\frac{e(U+U_1-\phi)}{kT}}. \tag{11}$$

2D single-layer SL MoS_2 diffusion capacitance, assuming equal electron and hole lifespan when the potential barrier height is perturbed, that is, considering that $\tau_n = \tau_p = \tau$, we have the following expression for the diffusion capacity of a 2D monolayer SL MoS_2:

$$C = \frac{q^2 n_i^2 \tau}{2kTN_d}\left(\frac{D_p}{L_p} + \frac{D_n}{L_n}\right)\exp\left(\frac{q(U+U_1-\phi)}{kT}\right). \tag{12}$$

Using the expression (11) and (12), it is possible to obtain a graph of the applied voltage dependence of the 2D and 3D p-n junction diffusion capacitances located in a weak microwave field (Fig. 11).

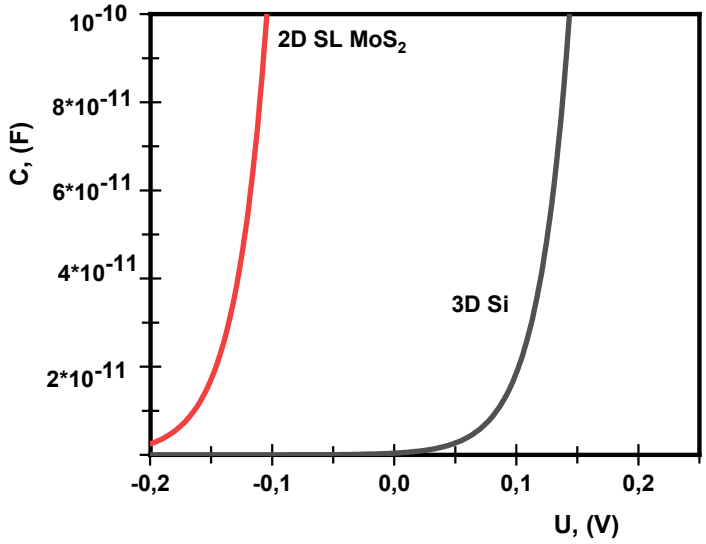

Figure 11. Dependence of the applied voltage of the 2D and 3D p-n junction diffusion capacitance located in a weak microwave field

As can be seen in Fig. 11, the theoretical calculations show that the diffusion capacity for 2D single-layer SL MoS_2 in the weak microwave field is greater than the 3D Si diffusion capacity.

We have the following expression for the differential conductance of a 3D-dimensional p-n junction under the influence of a strong microwave field:

$$C = \left(\left(\frac{kL_e\sqrt{TT_e}}{e^2 D_e n_p} e^{\frac{e(\phi_0-U_1-U)}{kT_e}-\frac{e\phi_0}{kT}}\right) + \left(\frac{kL_h\sqrt{TT_h}}{e^2 D_h p_n} e^{\frac{e(\phi_0-U_2-U)}{kT_h}-\frac{e\phi_0}{kT}}\right)\right)^{-1}\frac{\tau}{2}. \tag{13}$$

Electrons and holes in a 2D p-n junction are heated under the influence of a strong microwave field, taking into account the perturbation of the potential barrier height, the lifespan of electrons and holes are equal, that is, considering that $\tau_n = \tau_p = \tau$, in 2D size we have the following expression for the diffusion capacity of monolayer SL MoS_2:

$$C = \frac{q^2 n_i^2 \tau}{2kTN_d}\left(\frac{D_p}{L_p} + \frac{D_n}{L_n}\right)\left(\sqrt{\frac{T}{T_e}}\exp\left(\frac{q(\phi-U-U_1)}{kT_e} - \frac{q\phi}{kT}\right) + \sqrt{\frac{T}{T_h}}\exp\left(\frac{q(\phi-U-U_2)}{kT_h} - \frac{q\phi}{kT}\right)\right)^{-1}. \tag{14}$$

Using the expression (13) and (14), it is possible to obtain a graph of the applied voltage dependence of the diffusion capacity of a single-layer SL MoS_2 in 2D and 3D dimensions located in a strong microwave field (Fig. 12).

It can be seen from Fig. 12 that the diffusion capacity for 2D monolayer SL MoS_2 located in a strong microwave field is greater than the 3D Si diffusion capacity.

Using the expressions (10), (12) and (14), the variation of the 2D p-n junction diffusion capacitance under the influence of the microwave field is shown in Fig. 13.

The obtained results show that the 2D p-n junction diffusion capacity increases under the influence of a strong microwave field.

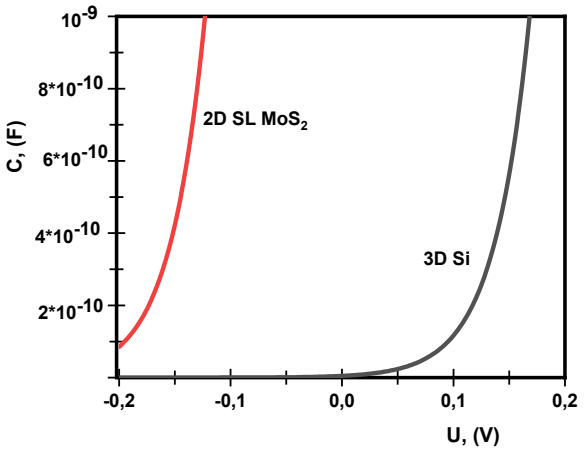

Figure 12. Dependence of the applied voltage of the 2D and 3D p-n junction diffusion capacitance located in a strong microwave field

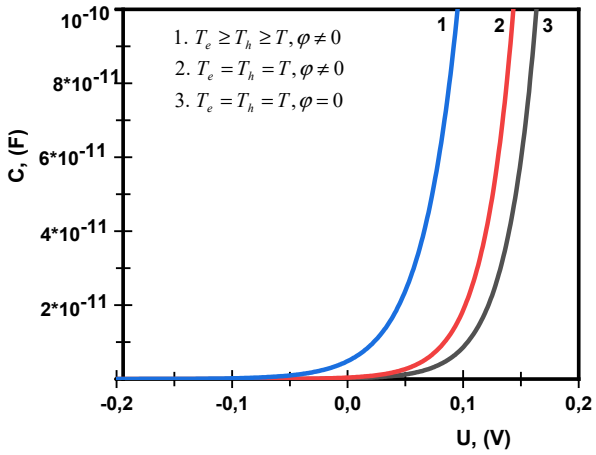

Figure 13. Voltage dependence of the diffusion capacity for a 2D single-layer SL MoS_2 in a strong microwave field

CONCLUSIONS

- The differential conductance of a 3D p-n junction is smaller than the differential conductance of a 2D p-n junction.
- The differential conductance of a 3D-dimensional p-n junction located in a weak and strong microwave field is small compared to the differential conductance of a 2D-dimensional p-n-junction. This shows that the 2D p-n junction located in weak and strong microwave field is more efficient than the 3D p-n junction.
- Theoretical calculations show that the diffusion capacity for 2D single-layer SL MoS_2 in both weak and strong microwave fields is greater than that of Si in 3D.
- The differential conductance and diffusion capacity of the 2D-sized p-n junction also increase under the influence of a strong microwave field.

ORCID

Muhammadjon G. Dadamirzayev, https://orcid.org/0000-0001-8258-4617
Mamura O. Kosimova, https://orcid.org/0000-0002-0759-5890; **Azamat S. Makhmudov,** https://orcid.org/0009-0001-1189-8202

REFERENCES

[1] T. Yang, B. Zheng, Z. Xu, T. Wang, C. Pan, J. Zou, X. Zhang, et al., "Van der Waals epitaxial growth and optoelectronics of large-scale WSe_2/SnS_2 vertical bilayer p–n junctions," Nat. Commun. **8,** 1906 (2017). https://doi.org/10.1038/s41467-017-02093-z
[2] Z. Lou, Z. Liang, and G. Shen, "Photodetectors based on two dimensional materials," Journal of Semiconductors, **37**(9), 091001 (2016). https://doi.org/10.1088/1674-4926/37/9/091001
[3] G. Gulyamov, U.I. Erkaboev, and A.G. Gulyamov, "Shubnikov–de Haas Oscillations in Semiconductors at the Microwave-Radiation Absorption," Adv. Cond. Matter Phys. **2019**, 3084631 (2019). https://doi.org/10.1155/2019/3084631
[4] R. Cheng, D. Li, H. Zhou, C. Wang, A. Yin, S. Jiang, anf X. Duan, "Electroluminescence and Photocurrent Generation from Atomically Sharp WSe_2/MoS_2 Heterojunction p–n Diodes," Nano Letters, **14**(10), 5590–5597 (2014). https://doi.org/10.1021/nl502075n
[5] H. Yuan, X. Liu, F. Afshinmanesh, W. Li, G. Xu, J. Sun, and Y. Cui, "Polarization-sensitive broadband photodetector using a black phosphorus vertical p–n junction," Nature Nanotechnology, **10**(8), 707–713 (2015). https://doi.org/10.1038/nnano.2015.112
[6] F. Wang, L. Yin, Z.X. Wang, K. Xu, F.M. Wang, T.A. Shifa, and J. He, "Configuration-Dependent Electrically Tunable Van der Waals Heterostructures Based on $MoTe_2/MoS_2$," Advanced Functional Materials, **26**(30), 5499–5506 (2016). https://doi.org/10.1002/adfm.201601349
[7] G. Gulyamov, G. Majidova, F. Muxitdinova, and S. Madumarova, "Changes in diodes with a pn-transition under the influence of microwave radiation," AIP Conference Proceedings, **2700**(1), 050008 (2023). https://doi.org/10.1063/5.0126385
[8] G. Gulyamov, F. Mukhitdinova, and G. Majidova, "Changing the Voltage of the p-n Junction in a Magnetic Field," e-Journal of Surface Science and Nanotechnology, **21**(4), 273-277 (2023). https://doi.org/10.1380/ejssnt.2023-047
[9] M.M. Furchi, A. Pospischil, F. Libisch, J. Burgdörfer, and T. Mueller, "Photovoltaic Effect in an Electrically Tunable van der Waals Heterojunction," Nano Letters, **14**(8), 4785–4791 (2014). https://doi.org/10.1021/nl501962c
[10] F. Wang, Z. Wang, K. Xu, F. Wang, Q. Wang, Y. Huang, and J. He, "Tunable GaTe-MoS_2 van der Waals p–n Junctions with Novel Optoelectronic Performance," Nano Letters, **15**(11), 7558–7566 (2015). https://doi.org/10.1021/acs.nanolett.5b03291
[11] C.H. Lee, G.H. Lee, A.M. van der Zande, W. Chen, Y. Li, M. Han, and P. Kim, "Atomically thin p–n junctions with van der Waals heterointerfaces," Nature Nanotechnology, **9**(9), 676–681 (2014). https://doi.org/10.1038/nnano.2014.150
[12] Y.J. Zhang, T. Oka, R. Suzuki, J.T. Ye, and Y. Iwasa, "Electrically Switchable Chiral Light-Emitting Transistor," Science, **344**(6185), 725–728 (2014). https://doi.org/10.1126/science.1251329
[13] A. Pospischil, M. Furchi, and T. Mueller, "Solar-energy conversion and light emission in an atomic monolayer p-n-diode," Nature Nanotech. **9,** 257–261 (2014). https://doi.org/10.1038/nnano.2014.14

[14] J.S. Ross, P. Klement, A.M. Jones, N.J. Ghimire, J. Yan, D.G. Mandrus, T. Taniguchi, et al., "Electrically tunable excitonic light-emitting diodes based on monolayer WSe_2 p–n junctions," Nature Nanotechnology, **9**(4), 268–272 (2014). https://doi.org/10.1038/nnano.2014.26
[15] M. Buscema, D.J. Groenendijk, G.A. Steele, H.S.J. van der Zant, and A. Castellanos-Gomez, "Photovoltaic effect in few-layer black phosphorus junctions defined by local electrostatic gating," Nature Communications, **5**(1), 4651 (2014). https://doi.org/10.1038/ncomms5651
[16] D. Li, M. Chen, Z. Sun, P. Yu, Z. Liu, P.M. Ajayan, and Z. Zhang, "Two-dimensional non-volatile programmable p–n junctions," Nature Nanotechnology, **12**(9), 901–906 (2017). https://doi.org/10.1038/nnano.2017.104
[17] J.-W. Chen, S.-T. Lo, S.-C. Ho, S.-S. Wong, T.-H.-Y. Vu, X.-Q. Zhang, Y.-D. Liu, et al., "A gate-free monolayer WSe_2 p-n-diode," Nature Communications, **9,** 3143 (2018). https://doi.org/10.1038/s41467-018-05326-x
[18] Z. Ni, L. Ma, S. Du, Y. Xu, M. Yuan, H. Fang, D. Yang, et al., "Plasmonic Silicon Quantum Dots Enabled High-Sensitivity Ultrabroadband Photodetection of Graphene-Based Hybrid Phototransistors," ACS Nano, **11**(10), 9854–9862 (2017). https://doi.org/10.1021/acsnano.7b03569
[19] D. Xiang, T. Liu, J. Xu, J.Y. Tan, Z. Hu, B. Lei, Y. Zheng, et al., "Two-dimensional multibit optoelectronic memory with broadband spectrum distinction," Nature Communications, **9**(1), 2966 (2018). https://doi.org/10.1038/s41467-018-05397-w
[20] Z. Hai, M.K. Akbari, Z. Wei, D. Cui, C. Xue, H. Xu, P.M. Heynderickx, et al., "Nanostructure-induced performance degradation of $WO_3 \cdot nH_2O$ for energy conversion and storage devices," Beilstein Journal of Nanotechnology, **9**, 2845–2854 (2018). https://doi.org/10.3762/bjnano.9.265
[21] U.I. Erkaboev, G. Gulyamov, J.I. Mirzaev, and R.G. Rakhimov, "Modeling on the temperature dependence of the magnetic susceptibility and electrical conductivity oscillations in narrow-gap semiconductors," International journal of modern physics B, **34**(07), 2050052 (2020). https://doi.org/10.1142/S0217979220500526
[22] J.O. Island, S.I. Blanter, M. Buscema, H.S.J. van der Zant, and A. Castellanos-Gomez, "Gate Controlled Photocurrent Generation Mechanisms in High-Gain In_2Se_3 Phototransistors," Nano Letters, **15**(12), 7853–7858 (2015). https://doi.org/10.1021/acs.nanolett.5b02523
[23] G. Gulyamov, U.I. Erkaboev, R.G. Rakhimov, and J.I. Mirzaev, "On temperature dependence of longitudinal electrical conductivity oscillations in narrow-gap electronic semiconductors," Journal of Nano-and Electronic Physics, **12**(3), (2020). https://doi.org/10.21272/jnep.12(3).03012
[24] E. Wu, Y. Xie, J. Zhang, H. Zhang, X. Hu, J. Liu, Ch. Zhou, et al., "Dynamically controllable polarity modulation of $MoTe_2$ field-effect transistors through ultraviolet light and electrostatic activation," Science Advances, **5**(5), eaav3430 (2019). https://doi.org/10.1126/sciadv.aav3430
[25] B.W.H. Baugher, H.O.H. Churchill, Y. Yang, and P. Jarillo-Herrero, "Optoelectronic devices based on electrically tunable p-n-diodes in a monolayer dichalcogenide," Nature Nanotechnology, **9**(4), 262–267 (2014). https://doi.org/10.1038/nnano.2014.25
[26] F.A. Chaves, P.C. Feijoo, D. Jiménez, "The 2D p-n-Junction Driven Out-of-Equilibrium," Nanoscale Advances, **2**, 3252-3262 (2020). https://doi.org/10.1039/D0NA00267D
[27] R.A. Smith, *Semiconductors*, first ed. (Cambridge University Press, 1959).
[28] G. Gulyamov, M.G. Dadamirzaev, and M.O. Kosimova, "Comparison of parameters of two-dimensional (2D) and three-dimensional (3D) pn-junction diodes," Romanian Journal of Physics, **68**, 603 (2023). https://rjp.nipne.ro/2023_68_1-2/RomJPhys.68.603.pdf
[29] G. Gulyamov; M.G. Dadamirzayev; M.O. Qosimova; and S.R. Boydedayev, "Influence of deformation and light on the diffusion capacity and differential resistance of the p-n junction of a strong electromagnetic field," AIP Conference Proceedings, **2700**, 050013 (2023). https://doi.org/10.1063/5.0124926

ПОРІВНЯННЯ ДИФЕРЕНЦІАЛЬНОЇ ПРОВІДНОСТІ ТА ДИФУЗІЙНОЇ ЄМНОСТІ 2D І 3D P-N ПЕРЕХОДУ

Мухамаджон Г. Дадамірзаєв, Мамура О. Косимова, С.Р. Бойдедаєв, Азамат С. Махмудов
Наманганський інженерно-будівельний інститут, Наманган 160103, Узбекистан

Під час виготовлення тривимірних p-n-переходів легування або модифікація поверхні, викликана ін'єкцією іонів, змінює електричні властивості та кристалічну структуру напівпровідника. Крім того, у міру зменшення розмірів напівпровідникового приладу в них поступово виникають різноманітні квантові ефекти. Це показує, що сфера застосування класичної теорії пристроїв зараз обмежена. Останніми роками великий інтерес викликають двовимірні (2D) матеріали з дивовижними атомарно тонкими властивостями. Властивості електростатичного поля деяких 2D p-n-переходів, таких як WS2, MoS2, MoSe2, WSe2 і чорний фосфор (BP), відкривають двері для нових можливостей для напівпровідників. Порівняно зміни дифузійної ємності та диференціальної провідності двовимірних p-n-переходів під впливом НВЧ-поля та дифузійних ємностей і диференціальної провідності двовимірних та тривимірних p-n-переходів під впливом НВЧ-поля.

Ключові слова: *p-n-перехід; дифузійна ємність; диференціальна провідність; мікрохвильове поле; двовимірні матеріали*